

Analysis of Stochastic Model in GEO/IGSO/MEO based on Triple-Frequency Observations

Xinjian Fang^{a,b}, Xuexiang Yu^{b,*}, and Chao Yan^b

^a*School of Earth and Environment, Anhui University of Science and Technology, Huainan, 232001, China*

^b*School of Geomatics, Anhui University of Science and Technology, Huainan, 232001, China*

Abstract

Focusing on the complex constellation of the BeiDou satellite navigation positioning system in China, this article analyzes the relationship between zero baseline and ultrashort baseline according to the residual value of carrier observation, signal to noise ratios, and elevation angles of different constellation satellites. A stochastic model based on the distance between the satellite and Earth, signal-to-noise ratio and elevation angle was proposed, which applied to the baseline solution of the Beidou triple-frequency single epoch. Analysis of measured data shows that compared with the traditional sinusoidal trigonometric function model, although the proposed model has no obvious effect on improving the positioning accuracy, the success rate of the ambiguity resolution of 4.2m, 4.17km and 8.84km are effectively improved by 0.1%, 4.7% and 1.1%, which enhanced the stability of calculation results.

Keywords: triple-frequency observations; single-noise ratio; carrier observation residuals; stochastic model

(Submitted on April 8, 2018; Revised on May 20, 2018; Accepted on June 11, 2018)

© 2018 Totem Publisher, Inc. All rights reserved.

1. Introduction

The BeiDou navigation satellite system (BDS) is a global satellite navigation system that is designed to meet the needs of national security and economic and social development. It is self-built, operated independently and is compatible with other satellite navigation systems in the world. It can be used by users all over the world and can provide weather, time, high-precision positioning, navigation, unidirectional and bidirectional time services and short message communication services. The space constellation of BDS is composed of geostationary earth orbit (GEO), inclined geosynchronous orbit (IGSO) and medium earth orbit (MEO) satellites, all of which transmit triple-frequency signals [10,11]. Compared with the GPS, GLONASS and GALILEO, the BDS has added GEO and IGSO satellites with high orbit and lower angular velocity.

Table 1. BD2 on-orbit statistics

Types	PRN	Track height	Launch date
GEO	C01	35786km	2010.01.17
	C02		2012.10.25
	C03		2010.06.02
	C04		2010.11.01
	C05		2012.02.25
	C17		2016.06.12
IGSO	C06	35786km	2010.08.01
	C07		2010.12.18
	C08		2011.04.10
	C09		2011.07.27
	C10		2011.12.02
	C13		2016.03.03
MEO	C11	21528km	2012.04.30
	C12		2012.04.30
	C14		2012.09.19

* Corresponding author.

E-mail address: xyu9166@aliyun.com

With the continuous development of BDS technology, requirements on real-time, dynamic, highly-efficient and reliable BDS results are getting higher and higher, and various effective and practical function models are constantly emerging. However, with the deepening of research, it is found that if we want to improve the accuracy of BDS to a greater extent, we must determine a reasonable stochastic model. Existing stochastic models can be mainly divided into four categories: equal weight stochastic model, stochastic model based on post-test residuals, satellite azimuth stochastic model and signal to noise ratio stochastic model [1,3,4,6,7,8,9,12]. Equal weight stochastic model does not accord with the actual situation. Under the condition that the multipath error and diffraction error have relatively large influences, the calculation results obtained by the equal weight model will be greatly offset from the true value. The stochastic model based on post-test residuals is a rigorous method for estimating variance-covariance of observations, but it is computationally intensive and not suitable for real-time calculations. The stochastic model based on satellite elevation angle and the stochastic model based on signal-to-noise ratio can precisely reflect the observed quality of observations to a certain extent.

In view of the complex constellation of BDS in China and the large difference between various types of satellites, the zero-baseline and ultra-short baseline data of Curtin University in Australia were used to analyze the relationship among the observed residuals, the signal-to-noise ratio and the elevation angle of different constellation satellites. A random stochastic model based on the combination of satellite-earth distance, signal-to-noise ratio, and elevation angle was proposed and applied to the baseline calculation of the BDS tri-frequency single epoch.

2. BDS Triple-frequency Observations Analysis and Determination of the Stochastic Model

2.1. Carrier Phase Observation Residual Analysis

Since two receivers are connected to the same antenna, they have the same multipath features, so the magnitude and characteristics of the observation noise can be well analyzed by a zero baseline. Ultra-short baselines can better eliminate error items such as satellite, receiver clock error and atmospheric delay, and their residuals are only affected by observation noise and multipath errors. Therefore, the magnitude of multipath can be effectively analyzed. The double difference observation equations between zero baselines and ultra-short baselines can be expressed as:

$$\lambda_i \nabla \Delta \varphi_i = \lambda_i \nabla \Delta N_i + \nabla \Delta \varepsilon_i \quad (1)$$

$$\lambda_i \nabla \Delta \varphi_i = \nabla \Delta \rho + \lambda_i \nabla \Delta N_i + \nabla \Delta \varepsilon_i \quad (2)$$

Where: λ represents carrier wavelength; $\nabla \Delta$ represents double difference observations; φ represents the carrier phase observation; N represents integer ambiguity; ρ represents satellite-earth distance and ε represents observational noise.

Use known coordinates and substitute the resolved ambiguities into double difference observation equations. Residual observations of the carrier at zero baselines and ultra-short baselines can be obtained.

The data came from Curtin University, Australia (<http://saegnss2.curtin.edu.au/ldc/>) Zero baseline CUT0-CUT2 and Ultra-short baseline CUT0-CUTB, and GPS for 12 time periods from November 2016 to October 2017 (one for each month) were selected. Each observation period lasted for 72 periods, with a 30-second sampling interval. The type of the receiver was Trimble NetR9. The data of zero baseline and ultra-short baseline were processed. Due to limited space, only the residual sequence analysis of the carrier phase observations in C01 (GEO), C07 (IGSO) and C12 (MEO) during the observation period of February 2017 (DOY:41-43) were selected. The reference satellites of both baselines were C03 (GEO). Fig. 1 and Fig. 2 show the residuals sequence of the carrier phase observations for the GEO, IGSO and MEO satellites in the zero and ultra-short baselines, respectively. In order to observe the relationship between the residuals observations of the carrier phase and the elevation angles, Fig. 3 shows the variation of the observed residuals of the carrier phase with the elevation angle of all the visible satellites in the 12 periods.

From Fig. 1, Fig. 2 and Fig. 3 we can see:

1) Different constellations of BeiDou satellites were observed at different times. The GEO satellites were observed for the longest period of time, mainly because the GEO satellites were geostationary satellites; The IGSO satellite is second because the IGSO is a regional service satellite whose projection of motion trajectory becomes "8" in the north and south relative to the Earth's equator; The MEO satellite is observed for the shortest period of time.

2) The residuals observed on the B1, B2, and B3 carrier phases of zero baseline GEO, IGSO and MEO are basically the same - all are within 20mm. The residuals observed on the B1, B2, and B3 carrier phases of ultra-short baseline GEO, IGSO

and MEO are less than 30mm. The residual error of the observation of the ultra-short baseline carrier phase is significantly larger than the zero baseline, which is mainly due to the multipath effect.

3) The fluctuations of the observed residuals of the carrier phase of GEO B1, B2 and B3 are small because the GEO satellite has a large elevation angle with little change. The observed residuals of B1, B2 and B3 in IGSO and MEO tended to decrease with an increase of elevation angle.

4) When the satellite altitudes are the same, the residual magnitude of the observed values of the carrier phase of different satellites are different, and the descending order is GEO, IGSO and MEO.

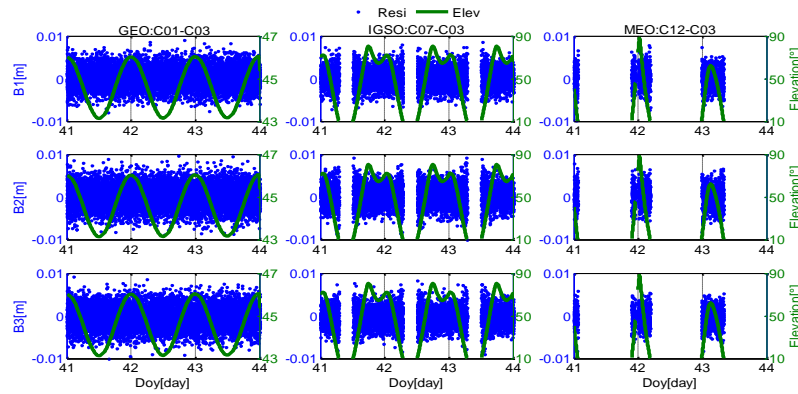


Figure 1. Zero baseline carrier observations residual sequence

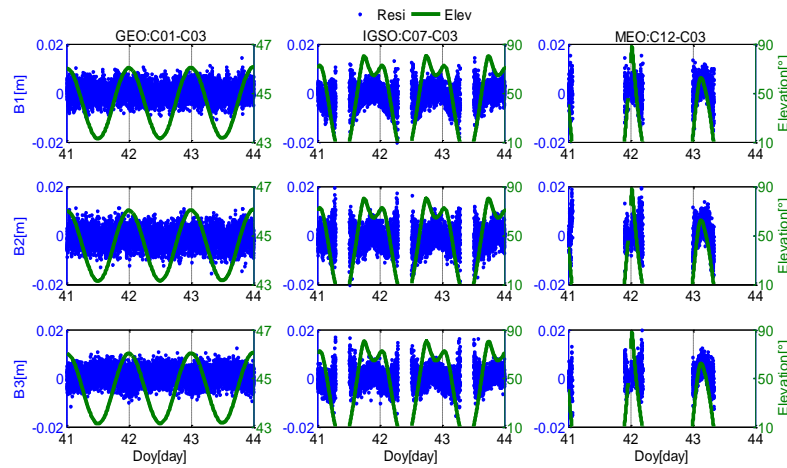


Figure 2. Ultra-short baseline carrier observations residual

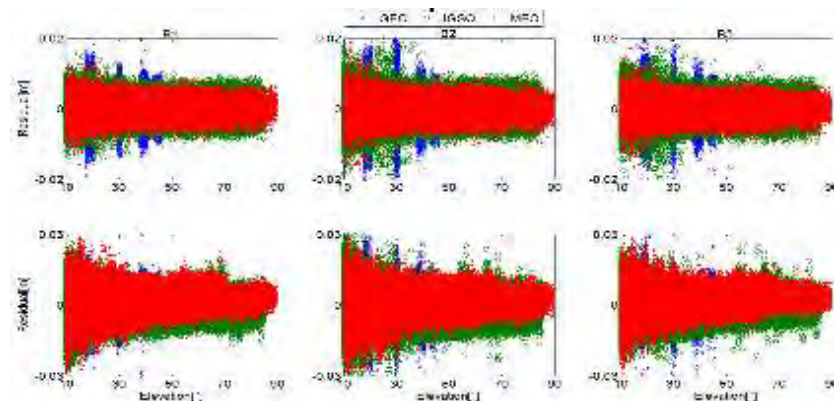


Figure 3. Variation of carrier observations with elevation angle (Upper: zero baseline; lower: ultra-short baseline)

2.2. Signal to Noise Ratio Analysis

Signal to noise ratio (SNR) can be used to measure the quality of ranging signals, and indirectly reflect the accuracy of ranging of carrier phases. BDS orbital satellites are complex in relation to each other, and all of them can transmit tri-frequency signals. By comprehensively using elevation angles and signal-noise ratios at different frequencies, the signal differences between different frequency points and different types of satellites can be well differentiated. Fig. 4 shows the changes of the signal to noise ratio between GEO, IGSO and MEO and B1, B2 and B3 of mobile stations CUT2 and CUTB with the elevation angle. Fig. 5 shows the signal-to-noise ratio between different frequencies, the relationship between the signal strength of the triple-frequency point and the elevation angle. Where $DSNR_{ij} = |SNR_i - SNR_j|$ represents the difference between the signal to noise ratio between i and j. The signal-to-noise ratio of satellites is generally 45 dBHz. The signal quality is good when the signal-to-noise ratio is large, and the signal strength $S_i = \text{int}(SNR_i / 5)$ ranges from 1 to 9.

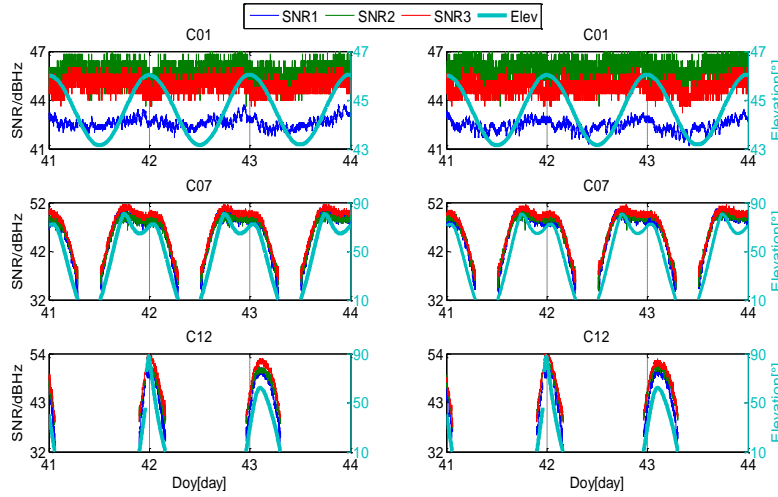


Figure 4. BDS signal-to-noise ratio with elevation angle changes (Left: CUT2 station; Right: CUTB station)

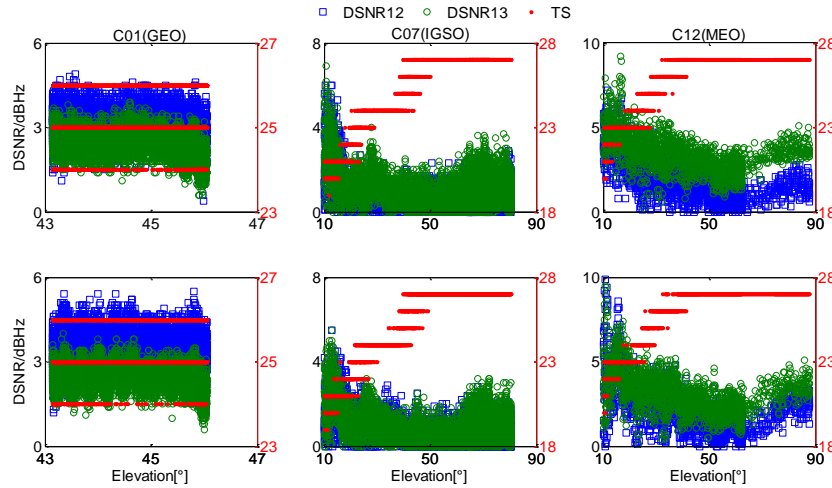


Figure 5. Relationship between SNR and elevation angle at different frequencies (Upper: CUT2 station; Lower: CUTB station)

In the picture, TS represents the sum of the signal strength of three frequency points. From Fig. 4 and Fig. 5 we can see:

1) SNR of BDS is related to satellite frequency. The SNR values of different frequencies of IGSO and MEO satellites have the same trend, that is, the SNR values of B1, B2 and B3 are consistent with the elevation angles. The larger the satellite elevation angle, the larger the SNR value, but the SNR values at B1, B2 and B3 are different. The SNR values and elevation angles of GEO satellites at different frequencies show no obvious regularity, which may be related to the fact that GEO satellites are geostationary satellites and the variation of elevation angle is small. The satellite signal-to-noise ratio of the three constellation satellites is between 32 and 55 dBHz, indicating that the observed signals of the observatory are good and the ionosphere activity is relatively stable.

2) The signal-to-noise ratio of various constellation satellites have a large difference, and the SNR difference between different frequency points of the GEO satellite is relatively stable. DSNR12 fluctuates around 4 and DSNR13 fluctuates around 3. IGSO satellites have smaller DSNR12 and DSNR13, which is obviously superior to the GEO satellite and MEO satellite. DSNR12 and DSNR13 of MEO satellites change frequently and have a large amplitude.

3) The sum of the signal intensities at tri-frequency points of different constellation satellites is quite different. There is no obvious regularity between the sum of signal intensities at the tri-frequency point of the GEO satellite and the elevation angle, and the value is between 24 and 26. The sum of the signal intensities of the three-frequency points of the IGSO satellite and the MEO satellite is consistent with the elevation angle. That is, the greater the satellite elevation angle, the greater the sum of the signal intensities at the tri-frequency point; its value is between 20 and 27.

Reference [4] pointed out that DSNR12 had the best effect when the threshold was 4, and DSNR13 had the best effect when the threshold was 3. Reference [9] pointed out that DSNR12 takes the best effect when the threshold value of 4 is taken, and DSNR13 takes the best effect when the value of 3 is the threshold value. So, based on the difference between the signal to noise ratio of different frequency points and the sum of the tri-frequency signal strength, the weighting factor f can be constructed:

$$f = \begin{cases} \frac{TS}{27}, & DSNR12 \leq 4, \\ \min\left(\frac{4}{DSNR12} \times \frac{TS}{27}, \frac{3}{DSNR13} \times \frac{TS}{27}\right), & DSNR13 \leq 3; \\ other & other \end{cases} \quad (3)$$

2.3. Determination of the Stochastic Model

The elevation angle model uses the elevation angle to represent the variance-covariance of the carrier phase observations, and for the different elevation angles of different satellites, the errors related to propagation paths it receives are also different. In the stochastic model based on elevation angle, the smaller the satellite elevation angle, the larger the influence of those errors on the observations and the lower the measurement accuracy. Usually, the sine elevation angle is applied to determine the weight:

$$\delta^2 = a^2 + \frac{b^2}{\sin^2(el)} \quad (4)$$

Where: δ is the mean square error of the satellite's original observations; el is the satellite elevation angle; a , b are empirical coefficients.

The empirical values are given in Eq. (4) are calculated from the GPS observations. As GEO and IGSO satellites are added to the BDS, the results of a and b will be different. Fig. 6 shows the standard deviation and elevation angle of the BDS satellite carrier phase residuals observed in 12 observation periods of zero-baseline. According to the relationship between standard deviation and elevation angle, the values of a and b are fitted as shown in Table 2.

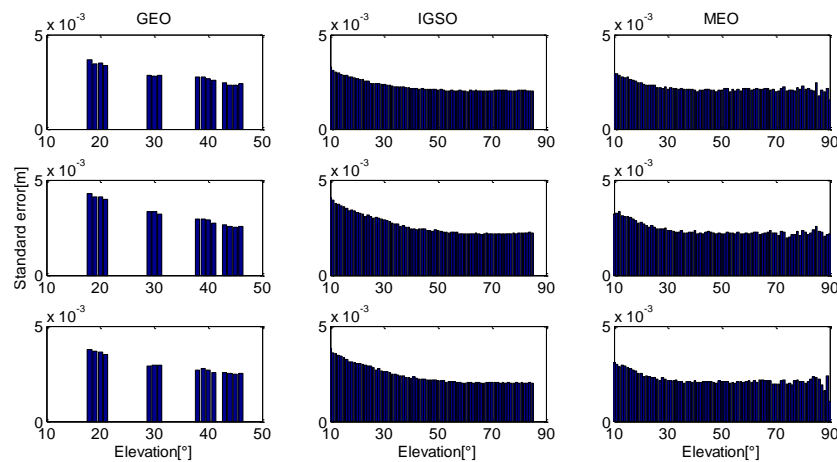


Figure 6. The variation of the standard deviation of the observed residuals of the waves with elevation angle (From top to bottom: B1, B2, B3)

Table 2. coefficient fitting value a, b(m)

Frequency	Coefficient	GEO	IGSO	MEO
B1	a	0.0020	0.0019	0.0020
	b	0.0010	0.0007	0.0003
B2	a	0.0017	0.0019	0.0021
	b	0.0014	0.0010	0.0005
B3	a	0.0021	0.0017	0.0020
	b	0.0010	0.0010	0.0004

Since the values at the three frequencies are very close, the sinusoidal elevation angle stochastic model for BDS is:

$$\sigma_B^2 = \begin{cases} 0.0020^2 + \frac{0.0010^2}{\sin^2(el)}, & GEO, \\ 0.0020^2 + \frac{0.0005^2}{\sin^2(el)}, & IGSO; \\ 0.0020^2 + \frac{0.0005^2}{\sin^2(el)}, & MEO; \end{cases} \quad (5)$$

Where: σ_B is the error in the original satellite observations fitted by the standard deviation of the observed residuals.

$$P = \frac{f}{\rho^2 \cdot \sigma_B^2} \quad (6)$$

3. Examples and Analysis

Three groups of baselines with different lengths, which are 4.2m ultra-short baseline, 4.17km short baseline, and 8.84km short baseline were adopted to carry out the test and analysis. Among them, data of the 4.2m ultra-short baseline comes from the measured data of GPS time October 11, 2017, by Curtin University, with a sampling interval of 30s. 2880 epochs were tested by the receiver, whose type was Trimble NetR9. The 4.17km and 8.84km short baseline were collected by a T300 GNSS receiver at Shannan New Area of Anhui University of Science and Technology, at GPS time of September 2017 with a sampling interval of 1 second and 3600 and 2000 epochs tested, respectively.

The BDS triple-frequency single epoch baseline solution function model is referred to reference [11]. For different stochastic models, the following test plan is designed:

Scheme one: Use Equation (4) to determine weight, where: $a=0.004$, $b=0.003$;

Scheme two: Use Equation (5) to determine weight;

Scheme three: Use Equation (6) to determine weight.

3.1. Ambiguity Solution Results Analysis

A single epoch ambiguity solution was carried out on the three groups of baselines based on the BDS triple-frequency single-epoch baseline solution described in [11]. The validity of the solution test can be measured by the success rate [2,5]. The 4.2m baseline applies the coordinates provided by the Curtin University GNSS Research Center in Australia as the reference value. The baselines of 4.17km and 8.84km take the data of the GNSS network of Shannan New Area of Anhui University of Science and Technology as the reference value. The fixed solution of each epoch is compared with the reference value. If they are the same, it is considered to be correct.

$$\text{Success rate} = \text{Correct fixed epochs} / \text{total epochs}$$

Table 3 shows the success rates of the three groups using different stochastic models.

Table 3. Ambiguity resolution success rate statistics of different schemes

Baseline	Model	Scheme		
		One	Two	Three
4.2m ultra-short baseline	Correct fixed epochs	2841	2844	2845
	Success rate/%	98.65	98.75	98.78
4.17km short baseline	Correct fixed epochs	3316	3346	3473
	Success rate/%	92.11	92.94	96.47
8.84km short baseline	Correct fixed epochs	1418	1507	1434
	Success rate/%	78.78	83.72	79.67

As seen from Table 3, with an increase of the baseline length, the success rate of ambiguity resolution decreases. Compared with the first scheme, the success rate of ambiguity resolution in the second scheme increased by 0.1%, 0.9% and 6.3%, respectively. That of scheme III increased by 0.1%, 4.7% and 1.1%, respectively. Therefore, the stochastic model proposed in this paper can better realize the single-epoch ambiguity resolution of BDS, which is better than the traditional sinusoidal trigonometric function model. It improves the success rate of ambiguity resolution and enhances the stability of the solution.

3.2. Positioning Accuracy Analysis

In the analysis of accuracy, this article only judges the correct ambiguity fixed epoch-solving results from the perspective of positioning results and compares that with the reference value. Fig. 7 shows the baseline deviations of the three baselines in the N (North), E (East) and U (Up) directions in the station coordinate system. In order to illustrate the positioning accuracy more directly, Table. 4 shows statistics of the three baselines in the N, E, U direction of the inner precision.

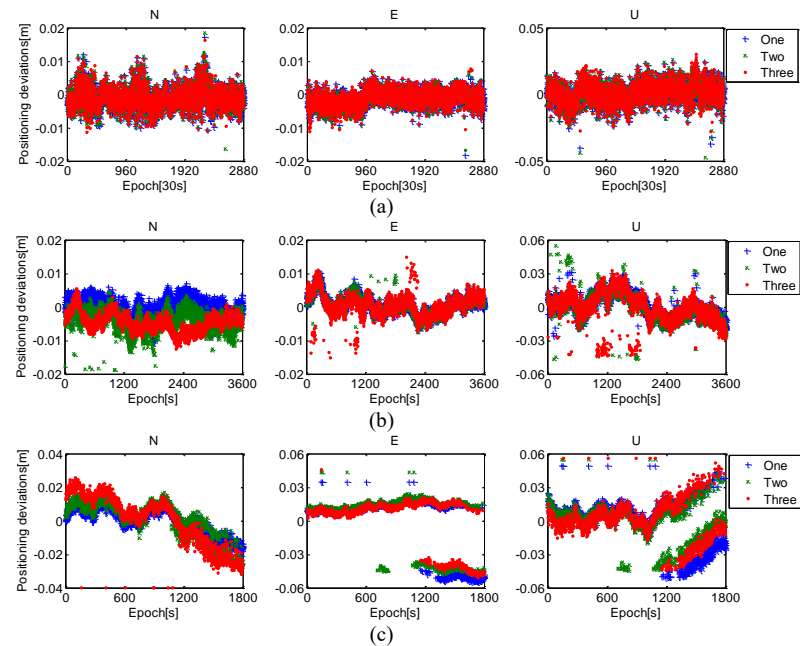


Figure 7. Positioning deviations of the three baselines in N, E and U directions

Table 4. Three baselines in the N, E, U direction inner precision of statistics (mm)

Baseline	N	E	U
4.2m ultra-short baseline	3.2	2.3	7.8
	3.2	2.3	7.5
	3.3	3.3	8.2
4.17km short baseline	4.0	6.0	10.7
	5.5	6.1	15.0
	6.3	5.4	18.3
8.84km short baseline	8.6	25.5	20.3
	12.0	25.0	16.5
	15.8	22.3	18.7

As seen from Fig. 7 and Table. 4, with the increase of the baseline length, the positioning accuracy decreases. This is because the short baseline double-difference may initially weaken some atmospheric errors such as partial ionosphere delay and tropospheric delay, but as the baseline increases, the residual error will lead to a larger position deviation. The accuracy of the 8.84km baseline in the E direction is significantly lower than that in the N and U directions, which may be the effect of a 12-storey building 50 meters away from the mobile station. Compared with the first scheme, the second scheme and the third scheme do not improve the positioning accuracy.

4. Conclusions

In view of the complex constellation of BDS in China and the large difference between different types of satellites, this paper analyzes the relationship between the observed residuals, signal-to-noise ratio and elevation angle of different constellation satellites at zero baseline and ultra-short baselines. According to the traditional sinusoidal trigonometric function model, this

paper proposes a stochastic model based on the combination of satellite-earth distance, signal-to-noise ratio and elevation angle, and verifies the success rate and accuracy of the ambiguity resolution with the measured data. The result shows that compared with the traditional sinusoidal trigonometric function model, although the stochastic model combines the satellite-earth distance, signal-to-noise ratio and elevation angle could not improve the positioning accuracy. It obviously improves the success rate of the ambiguity resolution and enhances the stability of the solution. As the length of the baseline increases, the success rate of ambiguity resolution and the accuracy of positioning all decrease. This is because the double difference of the short baseline station can weaken the atmospheric error, such as partial ionosphere delay and tropospheric delay. However, as the baseline increases, the residual error will result in a fixed error of ambiguity and a large position deviation. Therefore, the effects of the combined range of satellite distance, signal-to-noise ratio and height angle on the baseline solution of the medium-long baselines and single epoch still need further studying.

Acknowledgements

This work was supported in part by projects grant from the National Natural Science Foundation of China (Grand No.41474026).

References

1. C. Cai, Y. Gao, "Modeling and assessment of combined GPS/GLONASS precise point positioning," *GPS solutions*, vol. 17, no. 2, pp. 223-236, 2013.
2. C. L. Deng, W. M. Tang, "Reliable Sing-epoch ambiguity resolution for short baselines using GPS/BeiDou system," *GPS Solutions*, vol. 3, no. 18, pp. 375-386, 2014.
3. T. Li, J. Wang, and D. Laurichesse, "Modeling and quality control for reliable precise point positioning integer ambiguity resolution with GNSS modernization," *GPS solutions*, vol. 18, no. 3, pp. 429-442, 2014.
4. Q. K. Liu, L. F. Sui, and G. R. Xiao, "A method of determining the weight matrix for BDS DCB resolution," *Journal of Geomatics Science and Technology*, vol. 32, no. 5, pp. 473-478, 2015.
5. J. N. Liu, C. L. Deng, and W. M. Tang, "Review of GNSS ambiguity validation theory," *Geomatics and Information Science of Wuhan University*, vol. 39, no. 9, pp. 1009-1015, 2014.
6. P. Li, X. Zhang, "Integrating GPS and GLONASS to accelerate convergence and initialization times of precise point positioning," *GPS solutions*, vol. 18, no. 3, pp. 461-471, 2014.
7. C. Shi, Q. Zhao, and Z. Hu, "Precise relative positioning using real tracking data from COMPASS GEO and IGSO satellites," *GPS solutions*, vol. 17, no. 1, pp. 103-119, 2013.
8. W. M. Tang, C. L. Deng, and C. Shi, "Triple-frequency carrier ambiguity resolution for Beidou navigation satellite system," *GPS solutions*, vol. 18, no. 3, pp. 335-344, 2014.
9. G. R. Xiao, L. F. Sui, and C. J. Liu, "A method of determining the weight matrix for BeiDou navigation satellite system single point positioning," *Acta Geodaetica et Cartographica Sinica*, vol. 43, no. 9, pp. 902-907, 2014.
10. Y. Yang, Y. Xu, J. Li, and C. Yang, "Progress and performance evaluation of Bei Dou global navigation satellite system: Data analysis based on BDS-3 demonstration system," *Science China Earth Sciences*, vol. 61, no. 5, pp. 614-624, 2018.
11. C. Yan, X. X. Yu, and W. Xu, "Comparison of the stochastic model for single-epoch baseline resolution of IGSO/GEO/MEO triple-frequency," *Metal Min*, vol. 2017, no. 10, pp. 52-58, 2017.
12. X. H. Zhang, L. L. Ding, "Quality analysis of the second generation Compass observables and stochastic model refining," *Geomatics and Information Science of Wuhan University*, vol. 38, no. 7, pp. 832-836, 2013.

Xinjian Fang is currently a doctoral student at the School of Earth and Environment, Anhui University of Science and Technology of China. His main research direction is GPS/BDS deformation monitoring, data processing and mine disaster monitoring.

Xuexiang Yu received his Ph.D. from Wuhan University of China. Currently, he is a professor and doctoral supervisor at Anhui University of Science and Technology. His main research interests are GPS deformation monitoring automation, mine spatial information technology, disaster monitoring, and forecasting. He has published more than 50 papers in the Journal of Southeast University, Journal of China University of Mining & Technology, Journal of Surveying and Mapping, and Journal of Wuhan University, collectively. He is also a member of the International Mine Surveying Association, the Mine Surveying Professional Committee of the China Institute of Surveying and Mapping, and the Anhui Institute of Surveying and Mapping.

Chao Yan is currently a Master's student at the Institute of Surveying and Mapping, Anhui University of Science and Technology of China. His main research interests are satellite navigation and positioning technology.